Molecular Psychiatry (2018) 23, 1666–1673
www.nature.com/mp

OPEN

ORIGINAL ARTICLE

Longitudinal changes of tau PET imaging in relation to hypometabolism in prodromal and Alzheimer's disease dementia

K Chiotis[1], L Saint-Aubert[1], E Rodriguez-Vieitez[1], A Leuzy[1], O Almkvist[1,2,3], I Savitcheva[4], M Jonasson[5,6], M Lubberink[5,6], A Wall[5,7], G Antoni[7] and A Nordberg[1,2]

The development of tau-specific positron emission tomography (PET) tracers allows imaging *in vivo* the regional load of tau pathology in Alzheimer's disease (AD) and other tauopathies. Eighteen patients with baseline investigations enroled in a 17-month follow-up study, including 16 with AD (10 had mild cognitive impairment and a positive amyloid PET scan, that is, prodromal AD, and six had AD dementia) and two with corticobasal syndrome. All patients underwent PET scans with [^{18}F]THK5317 (tau deposition) and [^{18}F]FDG (glucose metabolism) at baseline and follow-up, neuropsychological assessment at baseline and follow-up and a scan with [^{11}C]PIB (amyloid-β deposition) at baseline only. At a group level, patients with AD (prodromal or dementia) showed unchanged [^{18}F]THK5317 retention over time, in contrast to significant decreases in [^{18}F]FDG uptake in temporoparietal areas. The pattern of changes in [^{18}F]THK5317 retention was heterogeneous across all patients, with qualitative differences both between the two AD groups (prodromal and dementia) and among individual patients. High [^{18}F]THK5317 retention was significantly associated over time with low episodic memory encoding scores, while low [^{18}F]FDG uptake was significantly associated over time with both low global cognition and episodic memory encoding scores. Both patients with corticobasal syndrome had a negative [^{11}C]PIB scan, high [^{18}F]THK5317 retention with a different regional distribution from that in AD, and a homogeneous pattern of increased [^{18}F]THK5317 retention in the basal ganglia over time. These findings highlight the heterogeneous propagation of tau pathology among patients with symptomatic AD, in contrast to the homogeneous changes seen in glucose metabolism, which better tracked clinical progression.

Molecular Psychiatry (2018) **23,** 1666–1673; doi:10.1038/mp.2017.108; published online 16 May 2017

INTRODUCTION

The aggregation of abnormally hyperphosphorylated tau protein into paired helical filaments is a key aspect of the pathology of Alzheimer's disease (AD).[1] Both the regional distribution of tau pathology in the brains of patients with AD and the sequential staging of its progression have been extensively described in *post-mortem* studies.[2–5] These studies indicated, for the first time, that an early and relatively long preclinical phase of tau aggregation precedes the symptomatic stages of AD.[6,7] Despite this, the time course of tau pathology propagation, especially in relation to changes in the concomitant clinical and cognitive profiles of the individual patients, remains largely speculative because of the inherent limitations of *post-mortem* studies.

During the past 5 years, the development of tau-specific positron emission tomography (PET) tracers[8] has provided a valuable addition to the neuroimaging arsenal. THK5317 [*(S)*-THK5117], a well characterised tau-specific tracer,[9–11] showed high retention in patients with AD with a regional pattern matching that of the distribution of tau pathology described by *post-mortem* studies.[12] Cross-sectionally, high load of tau pathology, as measured with THK5317 PET, was associated with hypometabolism in restricted brain regions,[12] while more extensive associations were reported in patients with substantially greater cognitive impairment, as measured with another tau tracer.[13–15] Studies with a longitudinal, multimodal design will shed light on the spreading of tau pathology in AD, and allow investigating whether the temporal trajectories of tau aggregation and hypometabolism are closely associated, or whether this association becomes closer with disease progression.

The aggregation of tau into filaments is not exclusively restricted to AD pathology but is also found in the less frequent amyloid-β-free degenerative tauopathies. Case series have revealed high regional retention of the tau tracers in patients with clinical diagnoses of corticobasal syndrome (CBS), but the regional distribution in these cases was different from that in patients with AD.[12,16–18] The understanding of the *in vivo* propagation of the pathology in the different degenerative tauopathies, however, remains elusive.

The aim of this longitudinal, multimodal study was to assess the propagation of tau pathology (using [^{18}F]THK5317 PET) in a cohort of patients with AD and cases with CBS, and to examine the

[1]Department of Neurobiology, Care Sciences and Society, Center for Alzheimer Research, Translational Alzheimer Neurobiology, Karolinska Institutet, Stockholm, Sweden; [2]Department of Geriatric Medicine, Karolinska University Hospital Huddinge, Stockholm, Sweden; [3]Department of Psychology, Stockholm University, Stockholm, Sweden; [4]Department of Radiology, Karolinska University Hospital Huddinge, Stockholm, Sweden; [5]Radiology, Department of Surgical Sciences, Uppsala University, Uppsala, Sweden; [6]Department of Medical Physics, Uppsala University Hospital, Uppsala, Sweden and [7]Department of Medicinal Chemistry, Uppsala University, Uppsala, Sweden. Correspondence: Professor A Nordberg, Center for Alzheimer Research, Division of Translational Alzheimer Neurobiology, Department of NVS, Karolinska Institutet, Novum 5th floor, Huddinge 141 57, Sweden.
E-mail: Agneta.K.Nordberg@ki.se
Received 9 January 2017; revised 14 March 2017; accepted 4 April 2017; published online 16 May 2017

relationships between tau pathology and markers of glucose metabolism and cognitive performance over time.

MATERIALS AND METHODS

Study sample

Eighteen patients who had previously participated in baseline investigations volunteered to participate in a longitudinal, multimodal follow-up study after a median of 17 months (interquartile range = (15:18)) from baseline. All patients had been referred for memory assessment to the Memory Clinic at the Department of Geriatric Medicine, Karolinska University Hospital, Stockholm, Sweden. The procedures for clinical assessment and patient recruitment are detailed elsewhere.[12]

At baseline, six patients were diagnosed with AD dementia (that is, probable AD and a positive [^{11}C]PIB PET scan[19,20]), and 10 with prodromal AD (that is, amnestic multi-domain mild cognitive impairment and a positive [^{11}C]PIB PET scan[20,21]). Two patients with CBS (fulfilled clinical criteria for possible corticobasal degeneration[22]) were also recruited; one of the two presented with unclear clinical features and was diagnosed with mild cognitive impairment at baseline. At follow-up, all 18 patients underwent [^{18}F]THK5317 and [^{18}F]FDG PET imaging as well as thorough clinical and neuropsychological investigations, within a 2-month period. During the follow-up interval, four of the patients with prodromal AD developed AD dementia.

The study was approved by the regional human ethics committee in Stockholm, as well as by the radiation safety committee of Uppsala University Hospital, Sweden. All participants and their caregivers provided written informed consent prior to the investigation and all procedures performed were in accordance with the ethical standards of the institutional and national research committee and with the 1964 Helsinki Declaration and its later amendments, or comparable ethical standards.

Neuropsychological assessment

All patients underwent neuropsychological assessments at baseline and follow-up. This included assessment of global cognition using the Mini-Mental State Examination (MMSE), and of episodic memory using, among others, the Rey Auditory-Verbal Learning (RAVL) encoding subtest (encoding scores summed across five trials). The latter was selected for further analyses because performance on this subtest was not affected by floor effects in individuals with severe cognitive deficits. Individual performance results for the RAVL encoding subtest are expressed as *z*-scores, in comparison with results from a reference group of healthy controls.[23]

Image acquisition

At baseline, all participants underwent [^{18}F]THK5317, [^{11}C]PIB and [^{18}F]FDG PET imaging as well as a T1-MRI sequence. At follow-up, all participants underwent [^{18}F]THK5317 and [^{18}F]FDG PET imaging. For [^{18}F]THK5317 PET, 22 frames were acquired over 60 min starting simultaneously with intravenous injection of 217 ± 42 MBq. For [^{11}C]PIB PET, 24 frames were acquired over 60 min after intravenous injection of 256 ± 67 MBq. The [^{18}F]FDG PET scans were acquired with a 15-minute static acquisition, 30 min after injection of 3 MBq/kg.

Regions of interest

For regional quantification, we used regions of interest (ROIs) derived from a probabilistic atlas,[24] spatially warped in each patient's native T1-MRI space, after application of an individual grey matter mask, as previously described.[12] Our choice of ROIs was based on previously published cross-sectional data on tau PET imaging—[12,25] parahippocampal gyrus, fusiform gyrus, middle and inferior temporal gyrus, posterior cingulate cortex and orbitofrontal cortex for patients with AD, and putamen for patients with CBS. A composite isocortical ROI was created for quantifying [^{11}C]PIB retention.

Data analysis

Individual dynamic baseline and follow-up [^{18}F]THK5317 PET images were co-registered separately onto the individual T1-MRI image using PMOD v.3.5 software (PMOD Technologies, Adliswil, Switzerland). Region-based kinetic modelling with the reference Logan graphical method was applied to extract the regional distribution volume ratio (DVR) values, with cerebellar grey matter as a reference, as previously described.[10] Voxel-based modelling was also applied, to create parametric DVR images.

Summation images from 40- to 60-minute [^{11}C]PIB PET scans were created and co-registered onto the individual T1-MRI images using SPM8 software, as were [^{18}F]FDG PET images. Standard uptake value ratio (SUVR) images were created using the cerebellar grey matter as reference for [^{11}C]PIB and the pons for [^{18}F]FDG.

The annual rates of change of [^{18}F]THK5317 DVR retention (Δ_{DVR}/year) and [^{18}F]FDG SUVR uptake (Δ_{SUVR}/year) were calculated for every patient, using both ROI- and voxel-based methods, as follows: ((follow-up − baseline)/time interval between scans).

Statistical analysis

Comparisons between baseline and follow-up. Differences between baseline and follow-up assessments of cognitive performance were assessed using paired *t*-tests ($P < 0.05$). Changes in [^{18}F]THK5317 retention and [^{18}F]FDG uptake over time were assessed using voxel-based paired *t*-tests as implemented in SPM8 software, with the time interval used as covariate. A cluster threshold of 20 voxels was applied, with no correction for multiple comparisons ($P < 0.001$). The determination of the sample size was based on an earlier published, exploratory study with a similar tau PET tracer.[26]

To account for the inter-individual variability in spreading of [^{18}F]THK5317 retention in our sample, tau spreading indices were calculated for every patient with AD ($n = 16$; Supplementary Figure 1). In brief, binary tau pathology maps were created for every patient at baseline and follow-up, based on the 90% confidence interval of tau distribution in healthy controls.[12] The subtraction of the baseline map from the follow-up map for each patient generated individual 'tau spreading indices'. Positive indices would illustrate that tau pathology in the cortex was overall spreading/expanding in an individual patient, and negative indices would illustrate an overall decrease of tau pathology distribution. A single sample *t*-test was applied to assess whether there was a significant spreading/reduction of tau pathology at a group level (that is, whether the tau spreading indices were significantly different from 0).

To find the ROIs in which [^{18}F]THK5317 retention increased over time, the proportion of patients in the AD groups (prodromal and dementia) in whom the annual rate of change was greater than the third quartile of the test–retest repeatability range for [^{18}F]THK5317[12] was determined for each region of the probabilistic atlas, and an ROI-based map was created with the results. The same analysis was not applied to the [^{18}F]FDG data due to the absence of [^{18}F]FDG test–retest measures in our study.

Comparisons between modalities. The relationships between the regional retention of [^{18}F]THK5317 at baseline and the rate of change in [^{18}F]THK5317 retention and [^{18}F]FDG uptake were assessed using the Pearson coefficient in the selected ROIs.

Linear mixed-effects models allowing for random intercepts between patients were employed to explore the relationship over time between regional [^{18}F]THK5317 retention and [^{18}F]FDG uptake as well as cognitive measures, with the time interval used as covariate. An additional linear mixed-effects model was applied to assess the relationship over time between [^{18}F]THK5317 retention and [^{18}F]FDG uptake across the four major brain lobes (frontal, temporal, parietal, occipital), similarly to the method from Ossenkoppele *et al*.[13] More specifically, [^{18}F]FDG uptake was assigned as the dependent variable, with [^{18}F]THK5317 retention, time point (baseline or follow-up) and their interaction as fixed factors, allowing for random intercepts across different patients and brain lobes (nested design). Simple slopes analyses were used to assess multiple linear regression two-way interactions.[27]

The cutoff point for statistical significance was $P < 0.05$. For statistical analyses involving multiple ROIs, both uncorrected and Bonferroni-adjusted (five ROIs) *P*-values are reported. For analyses involving cognitive tests, additional adjustments were performed (five ROIs and two cognitive tests). The data met the appropriate assumptions for the different statistical comparisons. All analyses were carried out using R v.3.3.1 software.

RESULTS

Clinical and neuropsychological profiles at follow-up in patients with AD

The characteristics of the study population are summarised in Table 1. MMSE scores were significantly lower ($P = 0.007$) at follow-

Table 1. Demographic and clinical characteristics of the study population; follow-up investigations were performed after a median of 17 months (interquartile range = (15:18))

Baseline diagnosis	*Prodromal AD* n = *10*	*AD dementia* n = *6*	*All patients with AD* n = *16*	*CBS* n = *2*
Developed dementia at follow-up	4	NA	4	1
Age at baseline (years)	65.0 (69.0:74.0)	68.5 (64.8:73.0)	70.5 (66.0:76.0)	69; 79
Gender (m/f)	4/6	1/5	5/11	2/0
ApoE ε4 carriers/non–carriers	6/3	5/1	11/4	0/1
Amyloid positive/negative ([^{11}C]PIB status)	10/0	6/0	16/0	0/2
Education (years)	12.0 (10.3:13.8)	14.5 (13.3:15.8)	13.0 (12.0:15.3)	15; 18
MMSE at baseline	28.0 (27.0:30.0)[a]	23.5 (23.0:24.8)[b]	26.0 (23.0:28.5)[c]	23; 27
MMSE at follow-up	26.0 (25.0:27.0)[a]	20.0 (16.3:23.8)[b]	25.0 (23.5:26.5)[c,d]	NA; 24
Episodic memory RAVL encoding subtest (*z*-scores) at baseline	− 1.8 (−2.1: − 0.5)[a]	− 2.5 (−2.6: − 2.4)[b,e]	− 2.1 (−2.3: − 0.9)[f]	− 1.8; − 1.0
Episodic memory RAVL encoding subtest(*z*-scores) at follow-up	− 1.8 (−1.9: − 0.8)[a]	− 2.1 (−2.5: − 2.1)[e]	− 1.8 (−2.1: − 1.4)[e]	NA; −2.3

Abbreviations: AD, Alzheimer's disease; ApoE, apolipoprotein E; CBS, corticobasal syndrome; f, female; m, male; MMSE, Mini-Mental State Examination; NA, not available; PIB, Pittsburgh compound B; RAVL, Rey Auditory-Verbal Learning; SUVR, standard uptake value ratio. Data are presented as medians (interquartile range) or as *n*. Mann–Whitney *U* and χ^2 tests were used to explore differences between patients with prodromal Alzheimer's disease and those with Alzheimer's disease dementia in terms of demographic information and cognitive performance. Prodromal AD = mild cognitive impairment with a positive [^{11}C]PIB PET scan (threshold SUVR of 1.41). [a]Data reported for nine patients who completed both baseline and follow-up investigations. [b]Significantly different from prodromal AD patients ($P < 0.05$). [c]Data reported for 15 patients who completed both baseline and follow-up investigations. [d]Significantly different from baseline ($P < 0.05$). [e]Data reported for three patients who completed both baseline and follow-up investigations. [f]Data reported for 12 patients who completed both baseline and follow-up investigations.

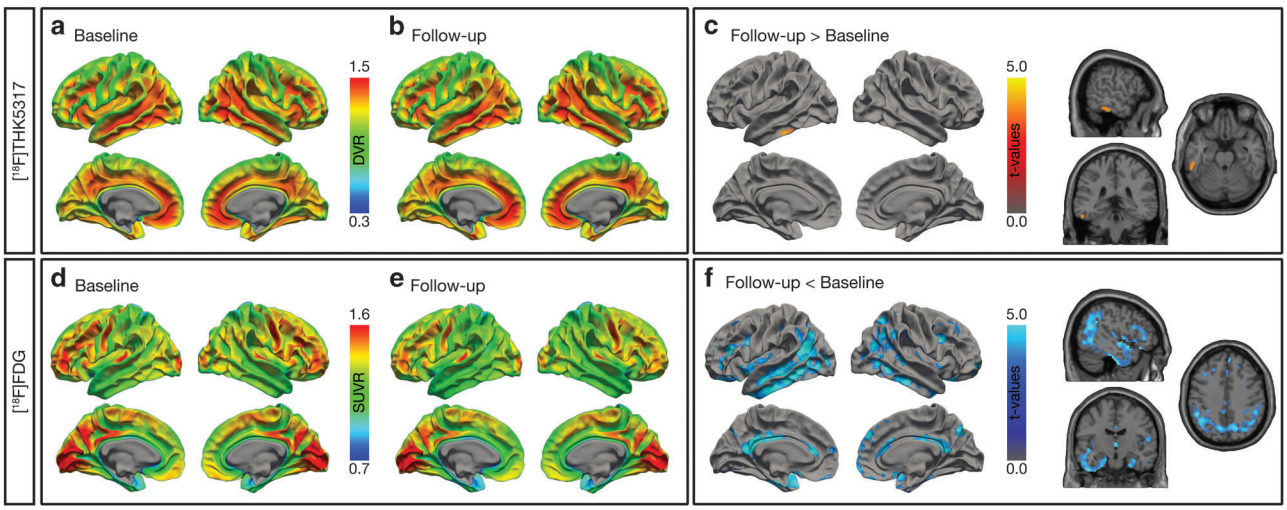

Figure 1. Average baseline and follow-up images from patients with AD (prodromal AD and AD dementia, $n = 16$), and projections of the results of voxel-based paired *t*-tests (SPM8 software) exploring the changes in retention/uptake over time for [^{18}F]THK5317 (**a**–**c**) and [^{18}F]FDG (**d**–**f**). A cluster threshold of 20 voxels was applied, with no correction for multiple comparisons ($P < 0.001$). AD, Alzheimer's disease; DVR, distribution volume ratio; SUVR, standard uptake value ratio.

up than at baseline in all patients with AD (prodromal and dementia); there were no statistically significant changes in RAVL encoding scores.

[^{18}F]THK5317 retention and [^{18}F]FDG uptake at follow-up in patients with AD

At baseline, across all patients with AD, high [^{18}F]THK5317 retention was predominantly observed in temporal, lateral occipital, and lateral and medial frontal areas (Figure 1a). The extent of retention remained visually the same at follow-up (Figure 1b), and voxel-based paired *t*-tests also detected no statistically significant increase in [^{18}F]THK5317 retention at follow-up, except for a focal area in the left inferior temporal gyrus (Figure 1c). Tau spreading index analyses revealed no spreading of [^{18}F]THK5317 retention over time at a group level. In contrast, low [^{18}F]FDG uptake was observed at baseline in temporoparietal areas, as seen in the average maps (Figure 1d), and this had clearly decreased at follow-up (Figure 1e). Indeed, statistical comparisons showed a significant decrease in [^{18}F]FDG uptake at follow-up, mainly in temporoparietal areas (Figure 1f).

To further explore possible changes in [^{18}F]THK5317 retention in the two AD groups separately (based on the baseline diagnosis), maps of the ROIs were created to illustrate the proportions of patients with increases in [^{18}F]THK5317 retention (annual rates) that were greater than those in the test–retest repeatability range. The areas in which the greatest proportion of patients showed substantial increase were the medial orbitofrontal cortex in patients with prodromal AD (Figure 2a) and the lateral occipital cortex in patients with AD dementia (Figure 2b). Overall, a substantial increase in [^{18}F]THK5317 retention in neocortical areas was observed more frequently in the AD dementia group than in the prodromal AD group (Figure 2).

Illustrative cases of patients with AD

Figure 3a illustrates the [^{18}F]THK5317 and [^{18}F]FDG PET scans at baseline and the maps of respective annual rates of change from

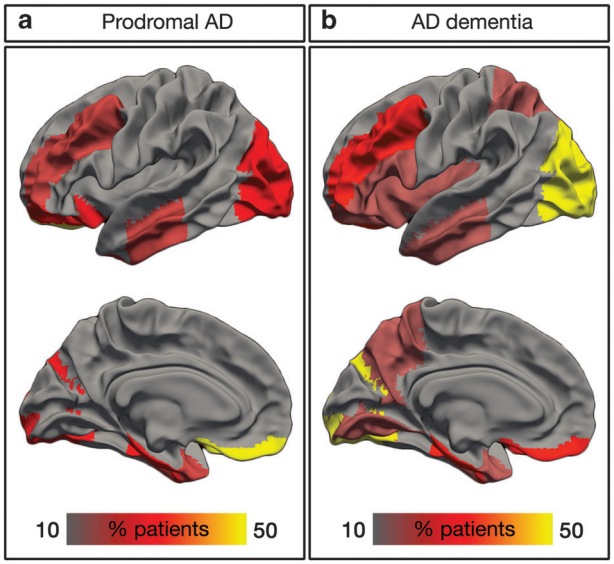

Figure 2. Regional maps illustrating the percentage (%) of patients with significant increase of annual [^{18}F]THK5317 retention in patients with (**a**) prodromal AD and (**b**) AD dementia. Significant increase was defined as annual rates of increase that were greater than the third quartile of the test–retest repeatability range.[12] AD, Alzheimer's disease.

two patients with a baseline diagnosis of prodromal AD and two with baseline diagnosis of AD dementia. With regard to the prodromal AD patients, case 1, who had milder cognitive impairment at baseline, had a stable diagnosis over time, while case 2 had developed AD dementia by follow-up. In the imaging profiles, case 1 had less [^{18}F]THK5317 retention at baseline but widespread increases in retention over time, while case 2 had only focal increases. With regard to [^{18}F]FDG PET, case 1 did not exhibit a clear hypometabolic pattern at baseline, and did not show substantial declines in tracer uptake over time. In contrast, case 2 had very low [^{18}F]FDG uptake in temporoparietal areas at baseline and further decreases in uptake at follow-up, mainly in temporal regions (Figure 3a).

With regard to the AD dementia patients, case 3 had milder cognitive impairment at baseline (as measured with MMSE) that remained stable over the follow-up interval, while the cognitive impairment in case 4 was worse at baseline and showed a clear further decline at follow-up (loss of seven points on MMSE). [^{18}F]THK5317 retention was less in case 3 than in case 4 at baseline but increased more over time compared with case 4. [^{18}F]FDG PET in case 3 showed relatively restricted areas with low tracer uptake than in case 4. [^{18}F]FDG uptake decreased widely in both cases with time, although this was more pronounced in case 4 (Figure 3a).

Relationships between [^{18}F]THK5317, [^{18}F]FDG and cognitive performance in AD

Significant negative correlations were observed between baseline [^{18}F]THK5317 retention and the rate of change of [^{18}F]THK5317 retention locally in the parahippocampal, fusiform and orbitofrontal cortex (Figure 4a). No significant correlations were observed between baseline local [^{18}F]THK5317 retention and the rate of change of [^{18}F]FDG in the selected ROIs.

There were no significant relationships over time between [^{18}F]THK5317 retention and [^{18}F]FDG uptake locally in the selected ROIs. Across the four major lobes, there was a significant effect of the interaction between [^{18}F]THK5317 retention and the time point (baseline or follow-up), on the [^{18}F]FDG uptake ($F = 5.505$, $P = 0.021$). Accordingly, the relationship between the two tracers showed significantly different slopes between baseline and follow-up (slope = − 0.202 and − 0.375, respectively) (Supplementary Figure 2).

Increased [^{18}F]THK5317 retention in the middle and inferior temporal gyrus significantly predicted decreased RAVL encoding scores but not MMSE scores (Figures 4b and c). No relationships were found between [^{18}F]THK5317 retention and cognitive performance (measured with MMSE or RAVL encoding tests) in the other ROIs. Decreased [^{18}F]FDG uptake in the middle and inferior temporal gyrus significantly predicted decreased MMSE and RAVL encoding scores (Figures 4b and c), while decreased [^{18}F]FDG uptake in the posterior cingulate gyrus predicted decreased MMSE scores (Supplementary Figure 3); however, the statistical significance of the RAVL encoding score predictions did not survive correction for multiple comparisons for any of the tracers in the selected ROIs.

[^{18}F]THK5317 retention and [^{18}F]FDG uptake at follow-up in patients with CBS

Both patients with a clinical diagnosis of CBS had a negative [^{11}C]PIB PET scan and high [^{18}F]THK5317 retention at baseline, with a regional distribution pattern that was distinct from the pattern of [^{18}F]THK5317 retention in patients with AD. High [^{18}F]THK5317 retention was detected predominantly in the basal ganglia, the thalami and the white matter, but also in isocortical areas, in these patients. Asymmetrical [^{18}F]FDG uptake was observed at baseline in isocortical areas, the basal ganglia and the thalami in both patients; however, the pattern of [^{18}F]FDG uptake was more asymmetrical in case 6 than in case 5 (Figure 3b).

At follow-up, measures of global cognition (MMSE) had substantially declined in both patients, in comparison to baseline (Table 1). Both also showed higher [^{18}F]THK5317 retention in the basal ganglia and isocortical areas than in the baseline investigations (Figures 3b and c). Case 6, who had higher MMSE scores and less white-matter retention at baseline, had more extensive retention in the same area at follow-up than case 5. Both patients had widespread areas of lower [^{18}F]FDG uptake in the isocortex at follow-up; case 6 showed the greatest changes in [^{18}F]FDG uptake over time (Figure 3b).

DISCUSSION

Thus far, our knowledge of the temporal evolution of tau pathology has been largely based upon either *post-mortem* studies[4,5] or theoretical models that have endeavoured to recapitulate the propagation of the pathology through cross-sectional tau PET imaging in mixed populations of patients and cognitively normal individuals.[28–30] In this study, we used [^{18}F]THK5317 PET imaging in a longitudinal, multimodal design to investigate *in vivo* the propagation of tau pathology in a cohort of patients with AD and cases with CBS, in relation to markers of glucose metabolism and cognitive performance.

The patients with AD who showed abnormally high [^{18}F]THK5317 retention in areas exceeding the limbic lobe at baseline[12] showed no significant increase in [^{18}F]THK5317 retention in the 17-month follow-up period, at a group level. A comparison of patients with prodromal AD and AD dementia, however, revealed different patterns of increases in [^{18}F]THK5317 retention. The medial orbitofrontal cortex, the area where greatest proportion of the prodromal AD patients showed increased [^{18}F]THK5317 retention, although outside the limbic lobe, shows extensive tau pathology in AD,[31] similar to the lateral temporal cortex,[32] and has been suggested as one of the isocortical regions early affected[5] due to its strong connections with the limbic system.[33–35] In contrast, the greatest proportion of the patients

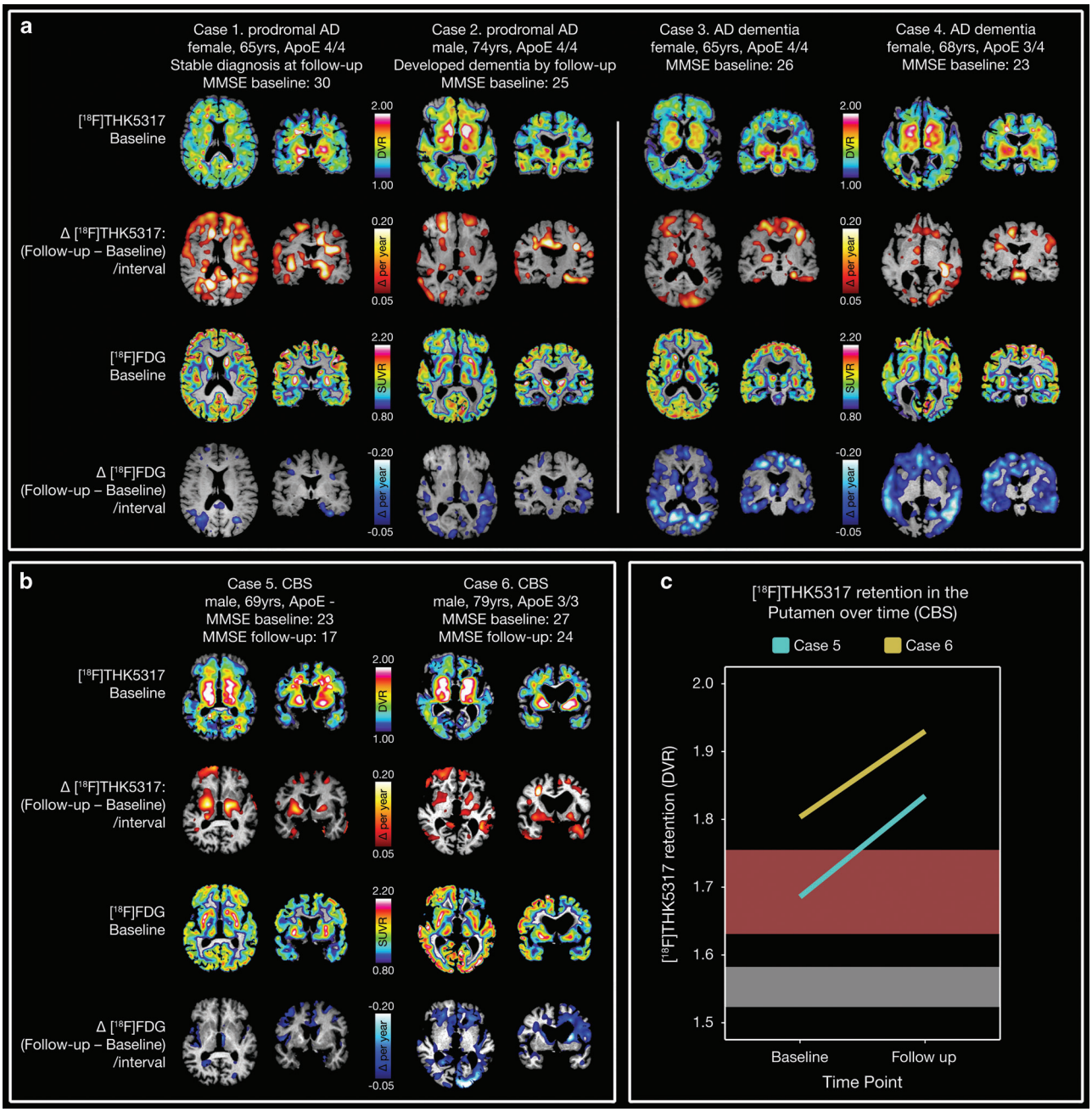

Figure 3. Imaging profiles from illustrative patients with baseline diagnoses of prodromal AD, AD dementia and CBS. [^{18}F]THK5317 (DVR) and [^{18}F]FDG (SUVR) PET scans at baseline and the maps of their respective annual rates of change are presented for each patient (**a**,**b**). (**c**) [^{18}F]THK5317 retention in the putamen in the two patients with CBS over time, plotted against the baseline retention values (interquartile range) from patients with AD ($n = 16$, brown ribbon) and those from young, healthy volunteers ($n = 5$, grey ribbon).[12] AD, Alzheimer's disease; Apo E, apolipoprotein E; CBS, corticobasal syndrome; DVR, distribution volume ratio; FDG, fluoro-deoxyglucose; MMSE, Mini-Mental State Examination; PET, positron emission tomography; SUVR, standard uptake value ratio.

with AD dementia showed increased [^{18}F]THK5317 retention in the association area of the occipital cortex, an area thought to be affected later in the disease progression.[5] Substantial changes in retention were not observed in the primary occipital cortex, an area affected at the last stage of tau spreading,[36] much later than its surrounding neocortex.[37,38] Finally, wide heterogeneity in the load and regional rates of change of [^{18}F]THK5317 retention was detected between individual AD patients even within each clinical group. It is therefore likely that patients clinically classified in the same group according to their functional impairment—namely, the prodromal and dementia stages of AD—were actually at different neuropathological stages and exhibited different patterns of tau propagation.

The extent of baseline [^{18}F]THK5317 retention in the parahippocampal and fusiform gyri and the orbitofrontal cortex, areas affected by tau pathology early in the time course of the disease, showed a negative correlation with the annual rates of change of [^{18}F]THK5317 retention. Despite the exploratory nature of this analysis, it is possible that the tau load in these areas could reach a critical value, after which the rate of accumulation would decelerate or even plateau, similarly to the changes in amyloid-β pathology early in the disease course.[39]

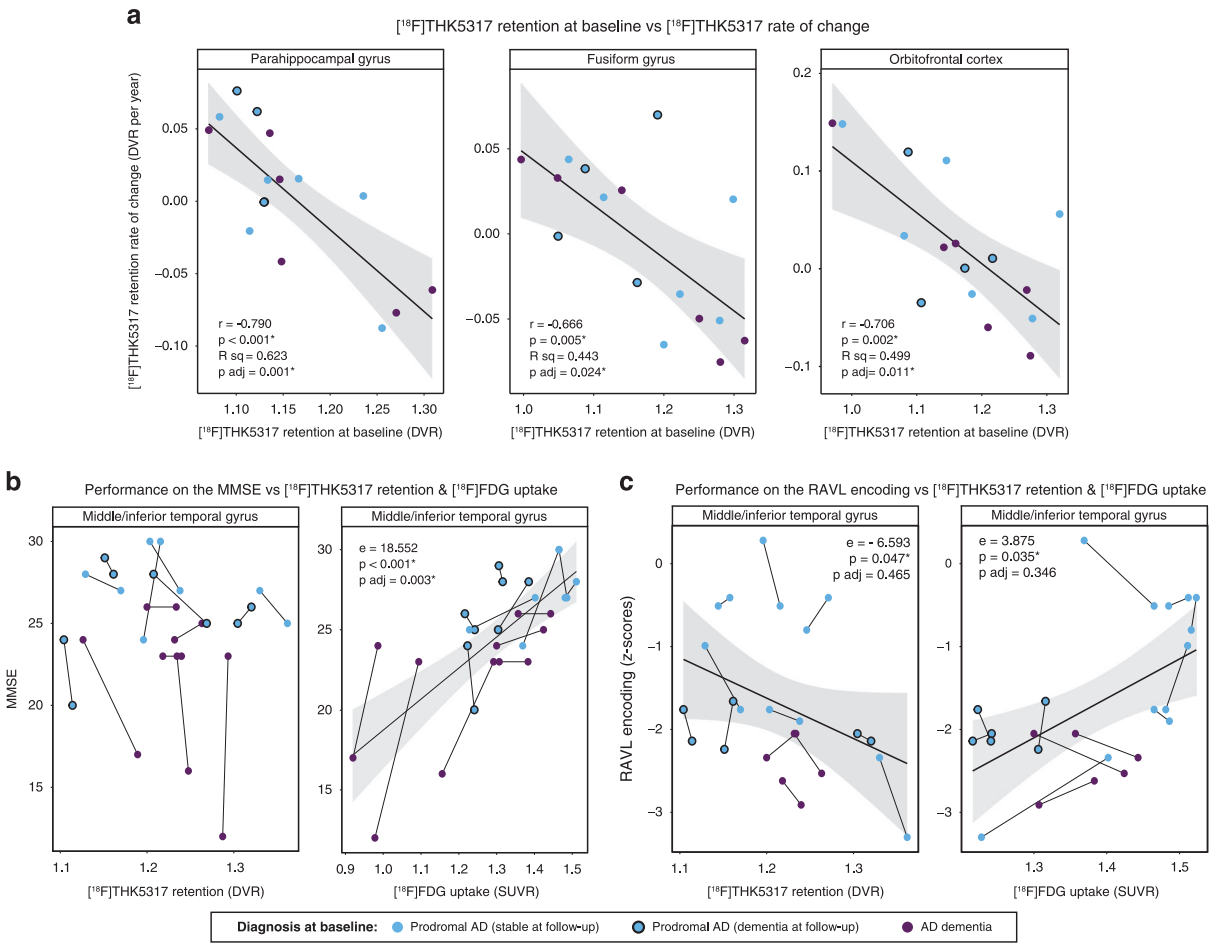

Figure 4. Relationship between [^{18}F]THK5317 retention, [^{18}F]FDG uptake and cognitive performance over time. More specifically, annual regional [^{18}F]THK5317 retention rate of change in relation to (**a**) local [^{18}F]THK5317 retention at baseline in the parahippocampal gyrus, fusiform gyrus and orbitofrontal cortex (Pearson's correlation analyses). Performance on (**b**) the MMSE and (**c**) the RAVL encoding tests in relation to the [^{18}F]THK5317 retention and [^{18}F]FDG uptake in the middle and inferior temporal gyrus over time (linear mixed-effects model analyses). The RAVL encoding performance results are expressed as *z*-scores. Linear mixed-effects model analyses were employed. AD, Alzheimer's disease; DVR, distribution volume ratio; e, estimate; FDG, fluoro-deoxyglucose; MMSE, Mini-Mental State Examination; *P* adj, Bonferroni-adjusted *P*-value; *r*, Pearson coefficient; R^2, coefficient of determination; RAVL, Rey Auditory-Verbal Learning; SUVR, standard uptake value ratio. *$P < 0.05$.

In contrast with the lack of changes in [^{18}F]THK5317 retention in patients with AD at a group level over the 17-month period, there were significant decreases in [^{18}F]FDG uptake in widespread areas of the temporoparietal cortex—a signature area for AD.[40] Interestingly, our data indicated the lack of a temporal association between changes in tau pathology and glucose metabolism, especially in areas affected early by tau. Based on the imaging profiles of the individual patients, it is conceivable that there may be a lag phase between the build-up of tau pathology and changes in glucose metabolism; during this phase, the neurons could tolerate a substantial amount of tau pathology,[41,42] possibly through endogenous compensatory mechanisms, before exhibiting metabolic changes. The latter would be consistent with cross-sectional findings indicating that the associations between markers of tau and metabolism become extensive in the dementia stage of the disease.[12,13,15,43] The existence of a lag phase is further supported by our analyses across the major brain lobes, where the relationship between tau pathology and hypometabolism proved closer with disease progression, when hypometabolism becomes more prevalent. The use of non-linear models in future studies with larger samples might be better suited to investigate the association between the two markers with time. Furthermore, longitudinal studies with adequate power, to study multi-level interactions, are warranted to investigate further the relationship between baseline tau pathology and the rate of change of glucose metabolism, as well as the possible synergistic effect of tau and amyloid-beta burden, as previously suggested.[14,44]

Global cognition (measured with MMSE) declined significantly in patients with AD; this decline correlated with decreased [^{18}F]FDG uptake but not with changes in [^{18}F]THK5317 retention over time. Changes in episodic memory correlated with changes in both longitudinal [^{18}F]FDG uptake (positively) and longitudinal [^{18}F]THK5317 retention (negatively); the correlations with episodic memory, however, did not survive correction for multiple comparisons and can be considered preliminary due to the small number of patients completing the episodic memory testing. The current data are in line with earlier cross-sectional findings[45] and support the notion that while tau deposition in the temporal cortex may be related to the earliest memory impairment, global cognitive changes are more closely related with hypometabolism in the relevant areas than with measures of tau propagation. Taken together, these findings hint that, in the symptomatic stages of AD, [^{18}F]FDG uptake and [^{18}F]THK5317 retention are not

tightly associated, and that [^{18}F]FDG PET might be a better tool for monitoring symptom progression.

At baseline, the patients with a clinical diagnosis of CBS showed a pattern of high [^{18}F]THK5317 retention and low [^{18}F]FDG uptake that was distinct from that in patients with AD, as previously described.[12,16–18] [^{18}F]THK5317 retention increased in both these patients over time, predominantly in the basal ganglia and frontotemporal areas, and [^{18}F]FDG uptake decreased isocortically. Nonetheless, there were differences between the two cases that might indicate that they were at different stages in the progression of the pathology. Notwithstanding the limitations of case studies, our findings illustrate the different regional distribution and progression patterns of tau pathology in patients with CBS, in contrast to patients with AD. More research in large groups of patients with CBS is required to determine: (1) whether the high binding of [^{18}F]THK5317 in the basal ganglia, which is dominant in both CBS and AD, would allow discrimination between the two, or if the assessment of AD-vulnerable regions would serve better this purpose; and (2) whether tau pathology monitors better disease progression in CBS in comparison to AD, as preliminarily observed in the profiles of our individual patients.

The results of this work are in contrast to the, so far, only longitudinal tau PET study published that reported changes in tracer retention over time.[26] We believe that this discrepancy could be attributed to the much smaller sample size of the latter study—five patients with AD dementia—as well as to the methodology used. In our cohort, the greater sample size increases the power of our calculations, and therefore increases the probability (positive predictive value) that our significant observed effects would reflect true effects, and not type I errors. Moreover, the use of dynamic data in a kinetic model-based approach to quantify [^{18}F]THK5317 retention (DVR) is another advantage of the current work, as DVR provide more accurate quantification of the tracer retention over time than late frame summation images (SUVR).[10]

The strength of this work lies in the longitudinal, multimodal design, which allowed the comparison between different clinical and imaging markers of the underlying pathology. The small sample size, however, is a clear limitation of the study, since it did not allow for separate inferential statistical analyses for the prodromal and AD dementia groups. Such analyses would probably provide additional information on the interrelationships between the markers. The processing of the follow-up data based on the baseline MRI, similarly to previous work,[46] represents another limitation, although the reported low rates of atrophy in isocortical areas at similar time intervals[47] would not be expected to have more than minimal effects given the spatial resolution of PET.

The interpretation of the observed relative stability in [^{18}F]THK5317 retention, at a group level, over time, however, is limited by our understanding of the tracer's binding. More specifically, the stability in retention could not exclude changes in the maturation status of the underlying tau deposits-preliminary evidence from *in vitro* studies suggests that the tracer binds to different types of tau deposits.[48]

In summary, this study suggests that patients in the symptomatic stages of AD exhibit heterogeneous regional load and propagation patterns of tau pathology over a 17-month period, despite being classified into similar groups of functional impairment. In direct contrast, glucose metabolism showed a more homogeneous pattern of decrease, which better tracked clinical progression. Our findings provide evidence of the lack of a linear relationship between tau pathology and more downstream markers, namely hypometabolism and measures of global cognitive impairment, during the course of the disease. Considerably more work is warranted to investigate tau propagation in larger sample sizes, at different stages of disease and using longer follow-up intervals, with special care around the possible uncoupling of clinical and neuropathological staging of AD.

CONFLICT OF INTEREST

The authors declare no conflict of interest.

ACKNOWLEDGMENTS

We express our gratitude to the patients and their relatives for making this study possible. We also thank Drs Vesna Jelic and Pia Andersen for their professional advice and support. We acknowledge the support from Professor Nobuyuki Okamura who kindly provided us with precursor for the synthesis of [^{18}F]THK5317. This study was financially supported by the Swedish Research Council (project 05817), the Swedish Foundation for Strategic Research (SSF), the Regional Agreement on Medical Training and Clinical Research (ALF) for Stockholm County Council, the Strategic Research Programme in Neuroscience at Karolinska Institutet, the Foundation for Old Servants, Axel Linder's Foundation, Gun and Bertil Stohne's Foundation, the KI Foundations, the Swedish Brain Foundation, the Swedish Alzheimer's Foundation (Alzheimerfonden), Demensfonden, the Wenner-Gren Foundations, the KTH-SLL grant and the EU FW7 large-scale integrating project INMiND (http://www.uni-muenster.de/INMiND).

REFERENCES

1 Hyman BT, Phelps CH, Beach TG, Bigio EH, Cairns NJ, Carrillo MC *et al.* National Institute on Aging-Alzheimer's Association guidelines for the neuropathologic assessment of Alzheimer's disease. *Alzheimers Dement* 2012; **8**: 1–13.
2 Braak H, Braak E. Neuropathological stageing of Alzheimer-related changes. *Acta Neuropathol* 1991; **82**: 239–259.
3 Hirano A, Zimmerman HM. Alzheimer's neurofibrillary changes. A topographic study. *Arch Neurol* 1962; **7**: 227–242.
4 Braak H, Del Tredici K. The pathological process underlying Alzheimer's disease in individuals under thirty. *Acta Neuropathol* 2011; **121**: 171–181.
5 Delacourte A, David JP, Sergeant N, Buee L, Wattez A, Vermersch P *et al.* The biochemical pathway of neurofibrillary degeneration in aging and Alzheimer's disease. *Neurology* 1999; **52**: 1158–1165.
6 Duyckaerts C, Hauw JJ. Prevalence, incidence and duration of Braak's stages in the general population: can we know?. *Neurobiol Aging* 1997; **18**: 362–369. discussion 389-392.
7 Nelson PT, Alafuzoff I, Bigio EH, Bouras C, Braak H, Cairns NJ *et al.* Correlation of Alzheimer disease neuropathologic changes with cognitive status: a review of the literature. *J Neuropathol Exp Neurol* 2012; **71**: 362–381.
8 Saint-Aubert L, Lemoine L, Chiotis K, Leuzy A, Rodriguez-Vieitez E, Nordberg A. Tau PET imaging: present and future directions. *Mol Neurodegener* 2017; **12**: 19.
9 Lemoine L, Saint-Aubert L, Marutle A, Antoni G, Eriksson JP, Ghetti B *et al.* Visualization of regional tau deposits using H-THK5117 in Alzheimer brain tissue. *Acta Neuropathol Commun* 2015; **3**: 40.
10 Jonasson M, Wall A, Chiotis K, Saint-Aubert L, Wilking H, Sprycha M *et al.* Tracer kinetic analysis of (S)-(1)(8)F-THK5117 as a PET tracer for assessing tau pathology. *J Nucl Med* 2016; **57**: 574–581.
11 Betthauser T, Lao PJ, Murali D, Barnhart TE, Furumoto S, Okamura N *et al. In vivo* comparison of tau radioligands 18F-THK-5351 and 18F-THK-5317. *J Nucl Med* 2016.
12 Chiotis K, Saint-Aubert L, Savitcheva I, Jelic V, Andersen P, Jonasson M *et al.* Imaging *in-vivo* tau pathology in Alzheimer's disease with THK5317 PET in a multimodal paradigm. *Eur J Nucl Med Molec Imaging* 2016; **43**: 1686–1699.
13 Ossenkoppele R, Schonhaut DR, Scholl M, Lockhart SN, Ayakta N, Baker SL *et al.* Tau PET patterns mirror clinical and neuroanatomical variability in Alzheimer's disease. *Brain* 2016; **139**: 1551–1567.
14 Bischof GN, Jessen F, Fliessbach K, Dronse J, Hammes J, Neumaier B *et al.* Impact of tau and amyloid burden on glucose metabolism in Alzheimer's disease. *Ann Clin Transl Neurol* 2016; **3**: 934–939.
15 Hanseeuw BJ, Betensky RA, Schultz AP, Papp KV, Mormino EC, Sepulcre J *et al.* FDG metabolism associated with tau-amyloid interaction predicts memory decline. *Ann Neurol* 2017.
16 Maruyama M, Shimada H, Suhara T, Shinotoh H, Ji B, Maeda J *et al.* Imaging of tau pathology in a tauopathy mouse model and in Alzheimer patients compared to normal controls. *Neuron* 2013; **79**: 1094–1108.
17 Josephs KA, Whitwell JL, Tacik P, Duffy JR, Senjem ML, Tosakulwong N *et al.* [18F] AV-1451 tau-PET uptake does correlate with quantitatively measured 4R-tau burden in autopsy-confirmed corticobasal degeneration. *Acta Neuropathol* 2016; **132**: 931–933.

18 Kikuchi A, Okamura N, Hasegawa T, Harada R, Watanuki S, Funaki Y *et al.* In vivo visualization of tau deposits in corticobasal syndrome by 18F-THK5351 PET. *Neurology* 2016; **87**: 2309–2316.
19 McKhann G, Drachman D, Folstein M, Katzman R, Price D, Stadlan EM. Clinical diagnosis of Alzheimer's disease: report of the NINCDS-ADRDA Work Group under the auspices of Department of Health and Human Services Task Force on Alzheimer's Disease. *Neurology* 1984; **34**: 939–944.
20 Dubois B, Feldman HH, Jacova C, Hampel H, Molinuevo JL, Blennow K *et al.* Advancing research diagnostic criteria for Alzheimer's disease: the IWG-2 criteria. *Lancet Neurol* 2014; **13**: 614–629.
21 Petersen RC, Smith GE, Waring SC, Ivnik RJ, Tangalos EG, Kokmen E. Mild cognitive impairment: clinical characterization and outcome. *Arch Neurol* 1999; **56**: 303–308.
22 Armstrong MJ, Litvan I, Lang AE, Bak TH, Bhatia KP, Borroni B *et al.* Criteria for the diagnosis of corticobasal degeneration. *Neurology* 2013; **80**: 496–503.
23 Bergman I, Blomberg M, Almkvist O. The importance of impaired physical health and age in normal cognitive aging. *Scand J Psychol* 2007; **48**: 115–125.
24 Hammers A, Allom R, Koepp MJ, Free SL, Myers R, Lemieux L *et al.* Three-dimensional maximum probability atlas of the human brain, with particular reference to the temporal lobe. *Hum Brain Mapp* 2003; **19**: 224–247.
25 Johnson KA, Schultz A, Betensky RA, Becker JA, Sepulcre J, Rentz D *et al.* Tau positron emission tomographic imaging in aging and early Alzheimer disease. *Ann Neurol* 2016; **79**: 110–119.
26 Ishiki A, Okamura N, Furukawa K, Furumoto S, Harada R, Tomita N *et al.* Longitudinal assessment of tau pathology in patients with Alzheimer's disease using [18F]THK-5117 positron emission tomography. *PloS ONE* 2015; **10**: e0140311.
27 Preacher KJ, Curran PJ, Bauer DJ. Computational tools for probing interactions in multiple linear regression, multilevel modeling, and latent curve analysis. *J Educ Behav Stat* 2006; **31**: 437–448.
28 Scholl M, Lockhart SN, Schonhaut DR, O'Neil JP, Janabi M, Ossenkoppele R *et al.* PET imaging of tau deposition in the aging human brain. *Neuron* 2016; **89**: 971–982.
29 Schwarz AJ, Yu P, Miller BB, Shcherbinin S, Dickson J, Navitsky M *et al.* Regional profiles of the candidate tau PET ligand 18F-AV-1451 recapitulate key features of Braak histopathological stages. *Brain* 2016; **139**: 1539–1550.
30 Cho H, Choi JY, Hwang MS, Kim YJ, Lee HM, Lee HS *et al.* In vivo cortical spreading pattern of tau and amyloid in the Alzheimer disease spectrum. *Ann Neurol* 2016; **80**: 247–258.
31 Van Hoesen GW, Parvizi J, Chu CC. Orbitofrontal cortex pathology in Alzheimer's disease. *Cereb Cortex* 2000; **10**: 243–251.
32 Price JL, Morris JC. Tangles and plaques in nondemented aging and "preclinical" Alzheimer's disease. *Ann Neurol* 1999; **45**: 358–368.
33 Laroche S, Davis S, Jay TM. Plasticity at hippocampal to prefrontal cortex synapses: dual roles in working memory and consolidation. *Hippocampus* 2000; **10**: 438–446.
34 Barbas H, Blatt GJ. Topographically specific hippocampal projections target functionally distinct prefrontal areas in the rhesus monkey. *Hippocampus* 1995; **5**: 511–533.
35 Kahn I, Andrews-Hanna JR, Vincent JL, Snyder AZ, Buckner RL. Distinct cortical anatomy linked to subregions of the medial temporal lobe revealed by intrinsic functional connectivity. *J Neurophysiol* 2008; **100**: 129–139.
36 Alafuzoff I, Arzberger T, Al-Sarraj S, Bodi I, Bogdanovic N, Braak H *et al.* Staging of neurofibrillary pathology in Alzheimer's disease: a study of the BrainNet Europe Consortium. *Brain Pathol* 2008; **18**: 484–496.
37 Pikkarainen M, Kauppinen T, Alafuzoff I. Hyperphosphorylated tau in the occipital cortex in aged nondemented subjects. *J Neuropathol Exp Neurol* 2009; **68**: 653–660.
38 McKee AC, Au R, Cabral HJ, Kowall NW, Seshadri S, Kubilus CA *et al.* Visual association pathology in preclinical Alzheimer disease. *J Neuropathol Exp Neurol* 2006; **65**: 621–630.
39 Jack CR Jr., Wiste HJ, Lesnick TG, Weigand SD, Knopman DS, Vemuri P *et al.* Brain beta-amyloid load approaches a plateau. *Neurology* 2013; **80**: 890–896.
40 Heiss WD, Kessler J, Szelies B, Grond M, Fink G, Herholz K. Positron emission tomography in the differential diagnosis of organic dementias. *J Neural Transm Suppl* 1991; **33**: 13–19.
41 de Calignon A, Spires-Jones TL, Pitstick R, Carlson GA, Hyman BT. Tangle-bearing neurons survive despite disruption of membrane integrity in a mouse model of tauopathy. *J Neuropathol Exp Neurol* 2009; **68**: 757–761.
42 Morsch R, Simon W, Coleman PD. Neurons may live for decades with neurofibrillary tangles. *J Neuropathol Exp Neurol* 1999; **58**: 188–197.
43 Dronse J, Fliessbach K, Bischof GN, von Reutern B, Hammes J, Kuhnert G *et al. In vivo* patterns of tau pathology, amyloid-beta burden, and neuronal dysfunction in clinical variants of Alzheimer's disease. *J Alzheimers Dis* 2016; **55**: 465–471.
44 Pascoal TA, Mathotaarachchi S, Mohades S, Benedet AL, Chung CO, Shin M *et al.* Amyloid-beta and hyperphosphorylated tau synergy drives metabolic decline in preclinical Alzheimer's disease. *Mol Psychiatry* 2017; **22**: 306–311.
45 Saint-Aubert L, Almkvist O, Chiotis K, Almeida R, Wall A, Nordberg A. Regional tau deposition measured by [18F]THK5317 positron emission tomography is associated to cognition via glucose metabolism in Alzheimer's disease. *Alzheimers Res Ther* 2016; **8**: 38.
46 Villemagne VL, Pike KE, Chetelat G, Ellis KA, Mulligan RS, Bourgeat P *et al.* Longitudinal assessment of Abeta and cognition in aging and Alzheimer disease. *Ann Neurol* 2011; **69**: 181–192.
47 Henneman WJ, Sluimer JD, Barnes J, van der Flier WM, Sluimer IC, Fox NC *et al.* Hippocampal atrophy rates in Alzheimer disease: added value over whole brain volume measures. *Neurology* 2009; **72**: 999–1007.
48 Harada R, Okamura N, Furumoto S, Tago T, Yanai K, Arai H *et al.* Characteristics of tau and its ligands in PET imaging. *Biomolecules* 2016; **6**: 7.

This work is licensed under a Creative Commons Attribution-NonCommercial-ShareAlike 4.0 International License. The images or other third party material in this article are included in the article's Creative Commons license, unless indicated otherwise in the credit line; if the material is not included under the Creative Commons license, users will need to obtain permission from the license holder to reproduce the material. To view a copy of this license, visit http://creativecommons.org/licenses/by-nc-sa/4.0/

© The Author(s) 2018

Supplementary Information accompanies the paper on the Molecular Psychiatry website (http://www.nature.com/mp)